Monitoring solutions for large movable scaffolding systems

André Resende, Hugo Coelho, Pedro Pacheco

Bridge Engineering Research and Design (BERD), Porto, Portugal

João Costa, Carlos Moutinho, Filipe Magalhães

Faculdade de Engenharia da Universidade do Porto (FEUP), Porto, Portugal

Contact: andre.resende@berd.eu

Abstract

This paper aims to describe the SMART-OPS research project, present preliminary results of the experimental campaign and foresee the characteristics and advantages of the product under development. In the first stage, a commercial monitoring equipment was adopted. The paper will describe preliminary results obtained with this equipment to demonstrate in a full-scale MSS under normal operation the advantages and challenges of monitoring. In the second stage, a customized monitoring system is under development.

The monitoring system was implemented in a Movable Scaffolding System (MSS) used to build spans up to 70m of prestressed concrete deck. The monitoring scheme included 2 sonic anemometers, 29 strain gages and 3 triaxial accelerometers. The MSS built 12 spans near Bratislava between May 2019 and February 2020.

Keywords: Movable Scaffolding Systems (MSS); Large MSS (LMSS); Organic Prestressing System (OPS); Structural Monitoring; Operational Modal Analysis (OMA).

1 Introduction

The 2.9km Danube Bridge is a highway crossing over the Danube River, 10km from the centre of Bratislava, Slovakia. The structure is part of a major highway project, which is being undertaken to ease traffic on existing radials and roads in and around the Slovak capital. The crossing comprises a 900m-long main bridge and two access viaducts: the 12-span 784m-long west viaduct and the 18-span 1,250.5m-long east viaduct.

For simplicity, the superstructure of the approach viaducts was built in two phases (see Figure 1). The first comprised the central box girder, which was built as a full span continuous beam using MSS. Lateral wings were built by wing travellers during the second phase. Both viaduct decks have similar cross sections and were designed to be built by similar MSS, both equipped with Organic Prestressing System (OPS) [1].

The construction of prestressed concrete bridge decks with MSS, a three-dimensional steel lattice structure that supports the formwork used to construct one entire span of the bridge deck that additionally has the ability to self-launch between adjacent spans, is normally used for a 40-60 m span range [2]. Until the last few years, bridges with 70-90 m spans were normally constructed with precast solutions, metallic solutions or balanced cantilever method.

Figure 1. Bratislava West approach viaduct construction: MSS on the front, building the deck central box and the wing traveller building the lateral slabs, on the back [3]

However, over the last few years, experiences have been made and new solutions have been developed for the 70-90m span range, usually referred as LMSS – Large MSS [4].

Unlike a permanent structure, MSS must undergo several operations with very different characteristics, namely:

- Static phase (usually called Concreting): suspension of the deck concrete weight while the deck is not self-supporting. The concrete weight is substantially bigger than the MSS weight. During this phase the MSS deformation is kept small by the OPS in order to achieve a bridge deck with the desired geometry;
- Movable phase (usually called Launching): movement of the MSS between adjacent spans facing an evolving structural system (the MSS moves above supports that run through the entire MSS length).

The OPS technology is an active control system for static or quasi-static loadings, where prestress cables and hydraulic jacks become part of the structure as structural members [1]. The hydraulic pressure in the jacks is controlled by an algorithm based on the mid-span deflection of the MSS. When the mid-span deflection reaches a predetermined threshold, the OPS algorithm transmits instructions to the hydraulic jacks which compensate the deflection (the algorithm induces force increment with increasing deflection).

While the OPS provided continuous and real-time control and monitoring for both MSS, a complementary monitoring system was installed exclusively on the MSS used for the construction of the 12-span west viaduct (53m + 10x67.5m + 53m). This complementary system is designed to gather data for treatment and analysis aiming the development of the OPS into a Smart_OPS, which can be applied broadly on MSS. The practical benefits are better knowledge of the behaviour of the MSS and the ability to make this information available in real-time to the operators and stakeholders at all phases of the working cycle.

The main goal of the SMART_OPS project is the development of a monitoring solution for large movable scaffolding systems (LMSS) with Organic Prestressing System (OPS). The OPS technology is expanding the use of MSS to much larger spans, being nowadays possible to use this technology to build spans with 90m [5]. This already highly technological machines will be equipped with a monitoring system that will permit to monitor online the forces transmitted to the supporting structure, the evolution of its response to strong winds and the tracking of its modal properties, with particular attention to the natural frequencies tracking, as a mean to detect structural anomalies and variations along MSS typical working cycle. The information supplied by the SMART_OPS provides also additional information to improve the safety and risk management in bridge construction.

The monitoring solution includes three subsystems, comprising 2 sonic anemometers, 3 triaxial accelerometers, 14 linear strain gages and 5 rectangular rosette strain gages.

The wind is the most important variable action for a MSS and the monitoring of wind characteristics provides validation of design assumptions and the correlation between the structural response and the excitation, to better define the interaction between the air flow and a flexible structure.

While the permanent loads were obtained by the sum of the weight of the individual elements, the static structural response was determined by measurement of strains on representative elements, and the dynamic response (vibration) was measured by accelerometers.

2 Anemometers Data

2.1 Sensors Layout

Both sonic anemometers (see Figure 2) were installed on the MSS between October 2019 and February 2020. In this first analysis, the data processing was limited to the first month, 01/10/2019 to 31/10/2019. The sonic anemometers provided information about 4 variables related with wind and temperature: Wind Speed, Wind Azimuth, Wind Elevation and Sonic Temperature. The anemometers sampling rate was around 28Hz but was adjusted in post-processing to 25Hz to ensure homogeneity. The results from both anemometers are similar, with minor differences in wind speed and wind direction. Therefore, in this presentation only the data from anemometer 2 is detailed.

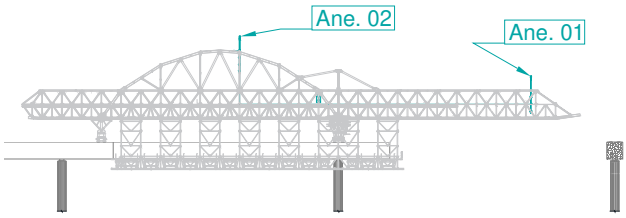

Figure 2. Anemometers positions

2.2 Wind Speed

The wind speed analysis is usually divided in 2 components: mean wind speed and turbulence. This is a viable approach if the period used to compute the mean speed falls on the spectral gap of wind speed auto-spectrum [6]. The existence of this spectral gap implies that the atmospheric movements in the mesoscale (mean speed component) and in the microscale (turbulence) are mutually independent and thus can be treated separately and the individual effects superimposed [6]. The choice of the averaging period is 10 minutes in many current standards, as the Eurocode [7]. This period is large enough to include the major part of wind speed short-duration fluctuation (turbulence) and sufficiently small so that the consecutive mean wind speeds are reasonably constant.

The mean wind speed for 10-minute periods reached 11.19m/s during October 2019 for the anemometer mounted 40m above the ground (see Figure 3).

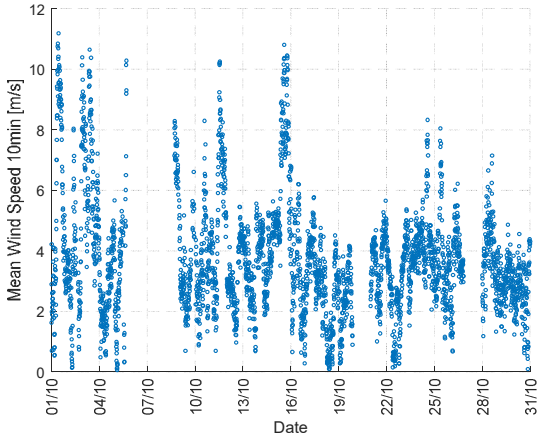

Figure 3. Mean wind speeds for 10-minute periods

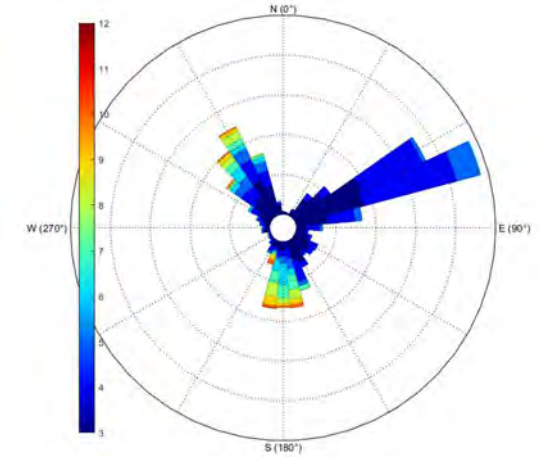

Figure 4. Wind azimuth and speed

The wind measured occurred in several plan directions, from which 3 were preponderant (see

Figure 4). The most frequent direction, around 70º with the North, is however the one with lower wind speeds. This direction is nearly the direction of the bridge deck and is possible that this wind direction is related with the preparation for bridge construction (the tree removal in the deck alignment created a channel of wind).

2.3 Wind Direction

The wind vector is projected in two different plans to define the azimuth and incidence angles. The azimuth is the angle between the North and the vector projected in the horizontal plan and the incidence angle is the angle between the horizontal plan with the projection of the wind vector in a vertical plan

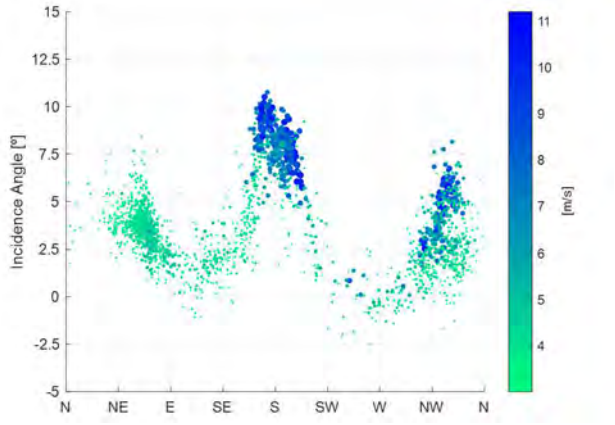

Figure 5. Wind azimuth, incidence and speed

The 3 preferred wind azimuths are 70º, 180º (wind from South) and 330º (wind between Northwest and North). The incidence angle represented in Figure 5 is almost always positive (ascending wind) which is expected as the MSS and the bridge under construction near the anemometers cause wind deviation to circumvent the obstacles.

2.4 Turbulence

The wind turbulence is usually described by the turbulence intensity, which is the ratio between the standard deviation of the turbulent component of the wind and the mean wind speed. In most cases the turbulence is characterized by 3 turbulence intensities in orthogonal directions: longitudinal aligned with the mean wind speed direction, transversal and vertical directions.

The longitudinal turbulence intensity is the highest, ranging from around 0.05 to 0.5, and reduces its spread with increasing wind speed. The mean value of longitudinal turbulence intensity for mean wind speeds larger than 3m/s was 0.218 (see Figure 6).

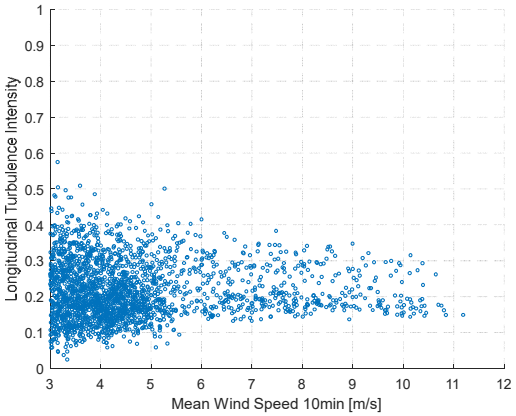

Figure 6. Longitudinal turbulence intensity

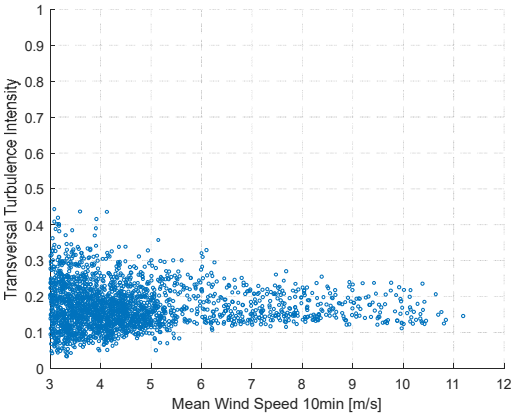

Figure 7. Transversal turbulence intensity

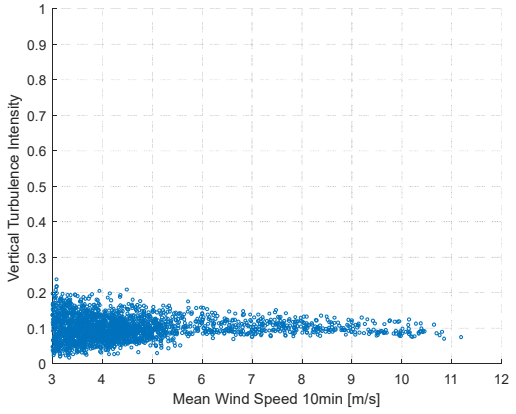

Figure 8. Vertical turbulence intensity

The transversal turbulence intensity ranges from 0.05 to 0.35 and the mean value is 0.173 (see Figure 7). Finally, the vertical turbulence intensity

is between 0.02 and 0.2 with mean value of 0.101 (see Figure 8).

The turbulence intensities are related and the typical ratios between them are presented for example in [6], where the value for the ratio between transversal and longitudinal turbulence intensities is 0.75 and the ratio between vertical and longitudinal turbulence intensities is 0.5. Considering only the mean values of turbulence intensity, in this application is obtained 0.79 for ratio transversal/longitudinal and 0.58 for the ratio vertical/longitudinal, which agree with typical values.

3 Strain Gages Data

3.1 Sensors Layout

In the first stage of the project, a commercial system was installed with 14 linear strain gages and 5 rectangular rosette strain gages, leading to a total of 29 measurement channels. This system was in operation between October 2019 and February 2020. Since the strain measurements are influenced by temperature, 17 resistance temperature sensors Pt100 were also installed. The temperature correction is made using known relations provided by the strain gage supplier for each sensor.

The strain gages positions were selected based on the MSS numerical model estimates in order to maximize the amount and quality of information. Aiming the demonstration of the principal results, in this presentation will be included only the results from 11 strain gages (see Figure 9).

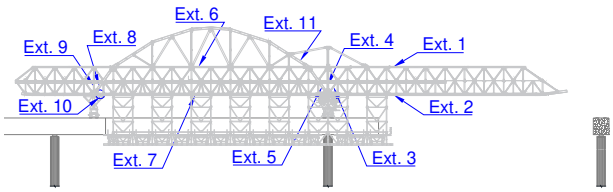

Figure 9. Strain gages positions

The sampling rate used for the strain gages was 50Hz and 1Hz for the Pt100.

3.2 Experimental vs Numerical Estimates

To compare the experimental results with the numerical estimates, the measurements of one complete deck span construction was selected (17 days between 02/10/2019 and 19/10/2019). In Figures 10 to 16 the stress evolution is presented for several strain gages [8]. The orange filling area of the Figures 10 to 16 is the static phase of the MSS operation and the blue filling area is the movable phase. Since the duration of the static phase is 16 days and the movable phase is only 1 day, the horizontal axis that represents time, was distorted in order to highlight the stress variations during the movable phase.

The strain gages measurements were converted to the correspondent stresses using the typical Mechanics of Materials relations [9]. The stresses are presented in [MPa].

The red line refers to the numerical model estimate, the blue line is the strain gage installed on the right lattice plane and the cyan line is the strain gage installed on the left lattice. Since the access to the left side of the MSS was difficult in some of the positions of Figure 9, in some cases the strain gages were installed only on the right lattice plan.

The stress variation is noteworthy, ranging from 261 MPa for the strain gage in position 3 to 114 MPa for the strain gage in the position 7.

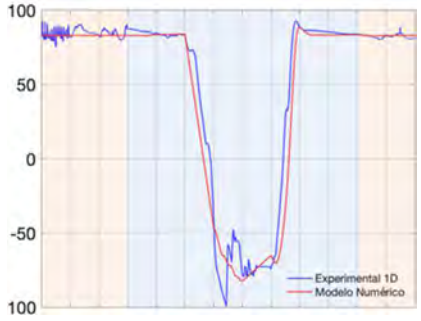

Figure 10. Stress evolution [MPa] for strain gage 1

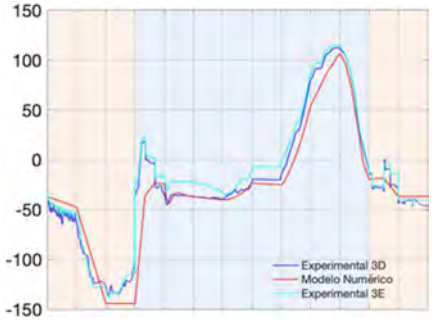

Figure 11. Stress evolution [MPa] for strain gage 3

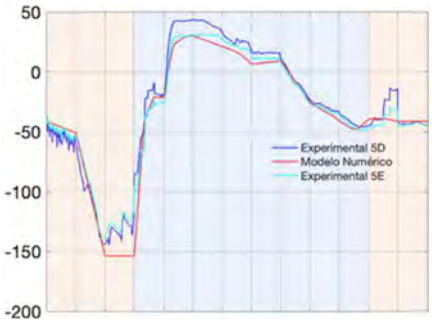

Figure 12. Stress evolution [MPa] for strain gage 5

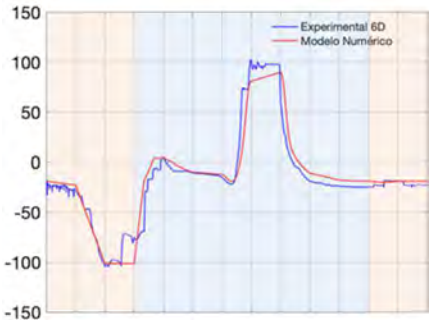

Figure 13. Stress evolution [MPa] for strain gage 6

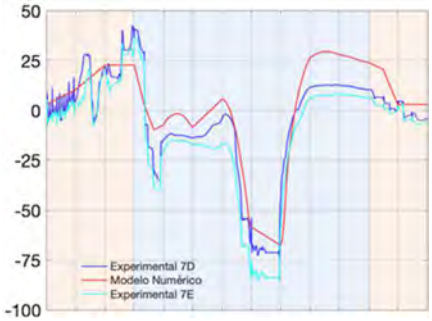

Figure 14. Stress evolution [MPa] for strain gage 7

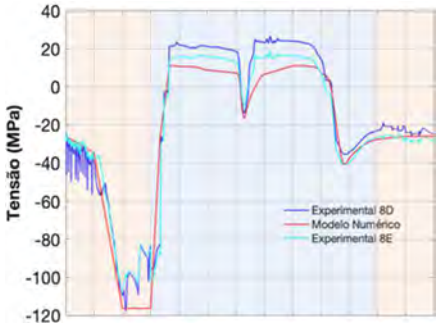

Figure 15. Stress evolution [MPa] for strain gage 8

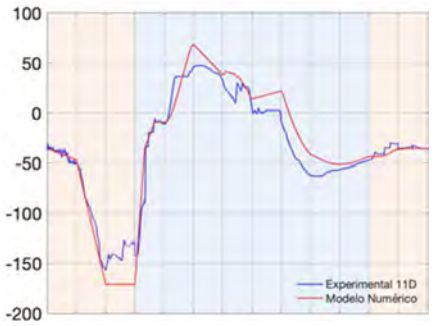

Figure 16. Stress evolution [MPa] for strain gage 11

The numerical model estimates match well the experimental results. However, there is still a little margin to investigate some discrepancies. This analysis is scheduled for the next stage of the SMART_OPS project.

4 Accelerometers Data

4.1 Sensors Layout

After some analyses on MSS numerical model to find the preferable positions for the accelerometers, an ambient vibration test was performed onsite. Finally, the elected positions include one at the tip of front cantilever (102), one near the middle of central span (103) and one at one-third of central span (104) (see Figure 17).

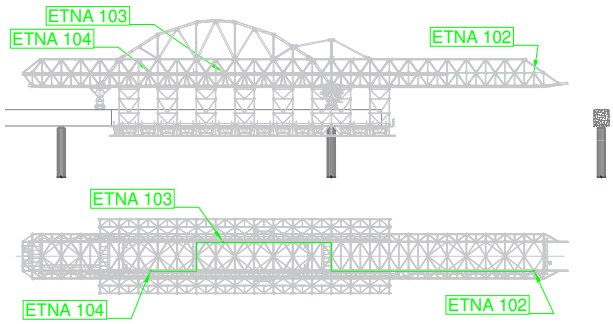

Figure 17. Accelerometers positions

Each of the 3 points is instrumented with triaxial accelerometers (longitudinal, transversal and vertical) measuring with a sampling rate of 50Hz.

The accelerometers were first installed in May 2019 and dismantled in February 2020. For demonstration purposes, in this publication only the data from July 2019 is included.

4.2 Vibration Level

The vibration levels in the transversal direction (see Figure 18) is very similar for the accelerometers in the MSS central span (103 and 104) and slightly higher for the one at the tip of front cantilever due to higher flexibility of the cantilever. The vibration level is also dependent on the existence of work onsite (14/07 in Figure 18 is a Sunday without work) and on the period of the day (the with higher vibration is near mid-day).

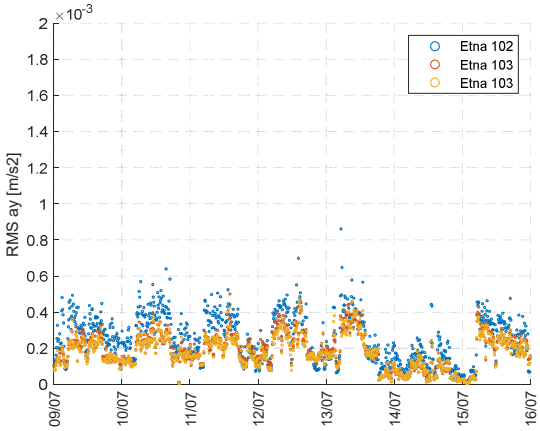

Figure 18. Vibration level in transversal direction

4.3 Modal Identification

After removal of long-term trends and decimation to 25Hz, each one-hour transversal and vertical data was subjected to a modal identification process using the Enhanced Frequency Domain Decomposition method (EFDD) [10].

Since the vibration levels are quite variable during the period under analysis, each spectrum is normalized by its maximum (consequently, the maximum of each spectrum is 1.0). This normalization hides the effect of different vibration levels on the spectrum but makes easier the identification of tendencies on the dominant frequencies' evolution. Figure 19 presents the normalized spectrum evolution, with red marking the highest values and blue marking the lowest.

The evolution presents several dominant frequencies identified in most of the spectra. The clearest example is the one near frequency 1.675Hz.

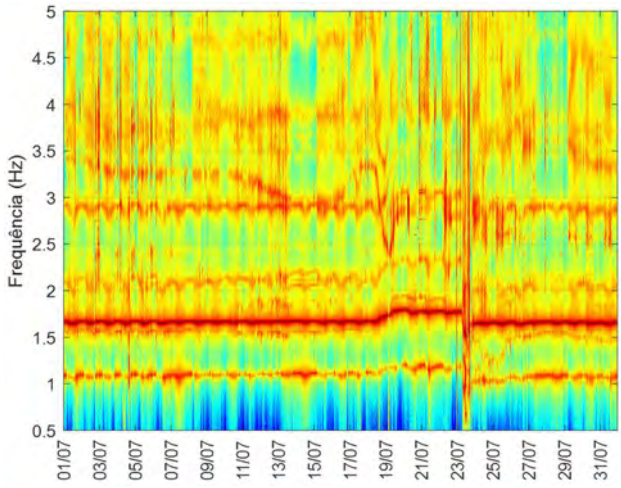

Figure 19. Colormap with spectra evolution during July 2019

Comparing the experimental results with their counterpart provided by the modal analysis of the numerical model, there are several frequencies that match very well (see Table 1). In this frequency comparison, to ensure the mode was the same for the experimental and numerical data, it was used the coefficient MAC (Modal Assurance Criterion) [11], ensuring that the MAC is at least 0.94 (the maximum MAC is 1.0 for superimposed modes).

Table 1. Comparison between Experimental and Numerical frequency modes

Mode	Experimental Frequency [Hz]	Numerical Frequency [Hz]	Ratio Exp. / Num. Freq.
1	1.092	1.082	99.1%
3	1.675	1.587	94.7%
4	2.078	2.071	99.7%
5	2.890	2.908	100.6%
6	3.196	3.416	106.9%
7	3.801	4.223	111.1%
8	4.292	4.555	106.1%

4.4 Frequency evolution during concrete hardening

In the spectra of Figure 19, it is visible an increasing step between 18/07 and 19/07, in a period that corresponds to the span concreting onsite. Therefore, the concreting and most specifically the concrete hardening implies an increment on the identified natural frequencies of

the MSS. The Figure 20 includes several one-hour data spectra along the concrete placement (the pouring takes around 27 hours).

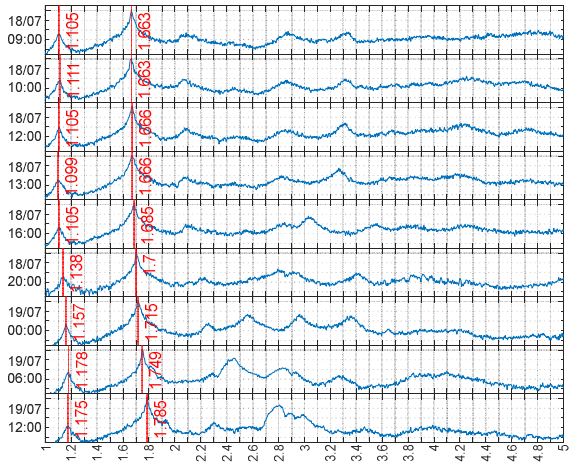

Figure 20. Spectra evolution during concreting

When the concrete span is able to self-support its weight, the MSS is disengaged and moved to the next span (happened on 23/07). After the reassembling of the MSS on the following span, the identified frequencies return to the ones verified before the concreting.

5 Conclusions

The monitoring system installed on the MSS consisting on anemometers, strain gages and accelerometers proved successful on verifying that the numerical models used in the design reflect well the MSS behaviour, since the comparison of stresses from the strain gages and identified vibration mode frequencies and shapes with the numerical counterpart showed very similar values. There is a little improvement margin that will be dealt with in the next phases of the project.

The wind characteristics were well identified, and the numerical models upgrade will consider the collected information.

6 Acknowledgments

This paper is a result of the project SMART_OPS – "Sistema de monitorização inteligente para equipamentos de grande dimensão usados na construção pontes", with the reference NORTE-01-0247-FEDER-033511, co-funded by European Regional Development Fund (ERDF), through North Portugal Regional Operational Programme (NORTE2020), under the PORTUGAL 2020 Partnership Agreement.

7 References

[1] Pacheco P., Guerra A., Borges P., Coelho H. Prestressing – the first of a new generation of structures. *SEI Reports* 4/2007

[2] SEOPAN *Manual de cimbras autolanzables*. Madrid: Tornapunta; 2015

[3] D4R7 Photogallery [Internet]. Jarovce - Ivanka Sever [cited 24 April 2020]. Available from: https://www.d4r7.com

[4] Pacheco P., Coelho H., Borges P., Guerra A. *Soluciones de Vanguardia para la Construcción de Puentes con Vanos de 70 a 90m*. Madrid: VI Congreso de ACHE; 2014

[5] Pacheco P., Coelho H., Borges P., Resende A., Carvalho D. New Frontiers in Multi-span Prestressed Concrete Deck Construction: A Case Study. *SEI* 2020

[6] Dyrbye C., Hansen S. *Wind Loads on Structures*. London: John Wiley & Sons; 1997.

[7] CEN *NP EN 1991-1-4 Eurocódigo 1 - Acções em estruturas Parte 1-4: Acções do vento*. Lisboa: IPQ; 2010

[8] Freitas J. *Ajuste de modelo numérico de cimbre baseado em resultados de monitorização*. Porto: MSC Thesis; 2020

[9] Gere J. *Mechanics of Materials*. Monterey: Brooks/Cole; 2001

[10] Magalhães F., Cunha A. (2011) *Explaining operational modal analysis with data from an arch bridge*. Mechanical Systems and Signal Processing, vol. 25; 2011

[11] Allemang R., Brown D. *A correlation coefficient for modal vector analysis*. Proceedings of the IMAC; 1982